STRide: a Framework to Exploit the Structure Information of Shareability Graph in Ridesharing Services

Yu Chen
East China Normal University
Shanghai, China
yu.chen@stu.ecnu.edu.cn

Peng Cheng
East China Normal University
Shanghai, China
pcheng@sei.ecnu.edu.cn

Lei Chen
The Hong Kong University of Science and Technology
Hong Kong SAR, China
leichen@cse.ust.hk

Wenjie Zhang
The University of New South Wales
Sydney, Australia
wenjie.zhang@unsw.edu.au

ABSTRACT

Ridesharing services play an essential role in modern transportation, which significantly reduces traffic congestion and exhaust pollution. In ridesharing problem, improving the sharing rate between riders can not only save the travel cost of riders and drivers, but also utilize of vehicle resources more efficiently. The existing online-based and batch-based methods for the ridesharing problem lack the analysis of the sharing relationship among riders. In addition, graph is a powerful tool to analyze the structure information between nodes. Therefore, in this paper, we propose a framework, namely STRide, to utilize the structure information to improve the results for ridesharing problems. Specifically, we extract the sharing relationships between riders to construct a shareability graph. Then, we define a novel measurement shareability loss for vehicles to select groups of requests such that the unselected requests still have high probabilities of sharing. Our SARD algorithm can efficiently solve dynamic ridesharing problem to achieve dramatically improved results. Through extensive experiments, we demonstrate the efficiency and effectiveness of our SARD algorithm on two real datasets. Our SARD can run up to 72.68 times faster and serve up to 50% more requests than the state-of-the-art algorithms.

PVLDB Reference Format:
Yu Chen, Peng Cheng, Lei Chen, and Wenjie Zhang. STRide: a Framework to Exploit the Structure Information of Shareability Graph in Ridesharing Services. PVLDB, 15(1): XXX-XXX, 2022.
doi:XX.XX/XXX.XX

PVLDB Artifact Availability:
The source code, data, and/or other artifacts have been made available at https://github.com/yuchenECNU/SARD.

Table 1: Requests Release Detail.

request	source	destination	release time	deadline
r_1	a	d	0	14
r_2	c	f	0	11
r_3	b	e	2	10
r_4	c	g	3	9

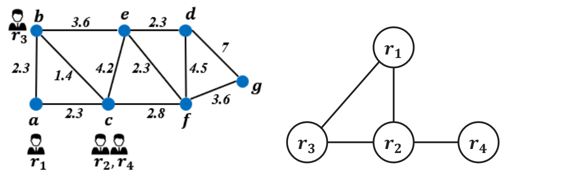

(a) Road Network (b) Shareability Graph

Figure 1: An Motivation Example

1 INTRODUCTION

Recently, ridesharing has become a popular public transportation choice, which makes a great contribution to reduce energy and relieve traffic pressure. In ridesharing, a driver can serve different riders simultaneously once riders can share parts of their trips and there are enough seats for them. The ridesharing service providers (e.g., Uber [3], Didi [2]) are constantly pursuing better service quality, such as higher servicing rate [17, 51], lower total travel distance [25, 37], or higher total revenue [6, 7].

For ridesharing platforms, *vehicle-request matching* and *route planning* are two critical issues to address. Given a set of vehicles and requests, vehicle-request matching filters out a set of valid candidate requests for each vehicle, while route planning targets on designing a route schedule for a particular vehicle to pick-up and drop-off the assigned requests.

If two requests can be served by any vehicle during the same trip, we call that they have a shareable relationship. Then, the shareable relationships between requests form a *shareability graph* of the requests, where each node represents a request and each edge indicates the connected two requests can share some part of their trips. The structure information of graphs can reveal many important properties (e.g., k-core [16, 35, 36, 47], k-truss [24, 45], clique [13, 21, 54]) and contribute to specific applications (e.g., community discovery [11, 12, 22], anomaly detection [43, 52], influential analysis [31, 32], etc). However, to the best of our knowledge, no existing works have targeted on utilizing the *structure properties* of the shareability graph to guide the vehicle-request matching to improve the service quality.

In this paper, we exploit the graph structures in shareability graph of requests to achieve better results for ridesharing services. In the sequel, we will illustrate our motivation with Example 1 as follows.

Proceedings of the VLDB Endowment, Vol. 15, No. 1 ISSN 2150-8097.
doi:XX.XX/XXX.XX

Example 1. *In a ridesharing example shown in Figure 1(a), there are four requests r_1, r_2, r_3, r_4 and a road network consisting of seven nodes $a \sim g$. The value close to each edge indicates the distance between the connected two nodes. The detailed information of requests is shown in Table 1, where the release time represents the time when the request is submitted to the platform, and deadline indicates the latest time to reach the destination. Suppose that the platform only allows a vehicle to serve at most two requests in a trip and it takes one unit of time to move one unit of distance in the road network. From the information given above, we have that r_1 can share with r_2 and r_3; r_2 can share with r_1 and r_3. But request r_4 can only share with r_2. We can construct a shareability graph of the four requests as shown in Figure 1(b), where each edge indicates the connected two requests can share with each other.*

If the platform uses an online assignment framework [25, 37, 44] for allocation (i.e., each request will be served or discarded immediately when it arrives), the platform will choose requests r_1 and r_2 to share a vehicle, which leads to that requests r_3 and r_4 cannot share with other requests anymore when they arrive.

Through investigating the shareability graph, the degrees of requests r_1, r_2, r_3, r_4 are 2, 3, 2, 1, respectively. In a shareability graph of requests, larger degree means more potential shareable requests. If we associate higher priorities to requests having lower degrees in the shareability graph (e.g., request r_4), we can get a better dispatch result: r_4 shares with r_1, and r_2 shares with r_3.

Therefore, the requests could be associated with different priorities to improve the service rate of the platform, which with higher priority will be arranged firstly to achieve a better objective.

In real platforms, vehicles and requests often arrive dynamically. Existing works on ridesharing can be summarized into two modes: the *online mode* [14, 20, 25, 37] and *batch mode* [5, 8, 53, 55]. The state-of-the-art operator for the online mode is *insertion* [14, 20, 44, 50, 55], which inserts the source and destination of a request into proper positions of the vehicle's route without reordering its current trip schedule such that the increase of the total travel cost is minimized. Batch-based methods [5, 39, 42, 53, 55] first package the incoming requests into groups, then assign a vehicle with a properly designed serving-schedule for each group of requests.

The existing approaches have their shortcomings. Insertion operator is very fast, but can only achieve the local optimal schedule for a request (e.g., minimized increase of travel cost). The batch-based methods can achieve better results (e.g., higher service rates or lower travel distances) than online methods for a period of relative long time (e.g., one day), but their time complexities are much higher than insertion (e.g., RTV needs to do bipartite matching, which is costly [5]). Can we have a more efficient batch-based approach to have better results for a relatively long time period (e.g., one day)?

In this paper, we propose a well-tailored batch-based framework, namely STRide, to exploit the structure information of requests' shareability graph in ridesharing systems such that the achieved results are significantly improved (e.g., higher service rates and lower travel distances) under just a slight delay of response time. *The key insight of our framework is to take the lead in integrating traditional allocation algorithm with graph analyses of the shareability graph in ridesharing problems.* In our STRide framework, we first propose a fast shareability graph builder, which efficiently extracts shareable relationships between requests through ellipse and angle-based filtering to only maintain the good shareable relationships (i.e., requests with close travel directions such that the detours of the serving vehicles are intuitively small). To exploit the structure information of shareability graph, we devised an efficient algorithm, namely *structure-aware ridesharing dispatch* (SARD), to take the cohesiveness of requests in shareability graph (evaluated through the structure information of the graph) into consideration and revise the priority of each request through analyzing its shareability in the assignment phase. SARD adopts a two-phase strategy of "proposal-acceptance", which avoids enumerating invalid groups for any specific vehicle. When we design a schedule for a vehicle to serve a set of riders, we adjust the insertion order of riders' requests based on the requests' shareability in the shareability graph, such that the maintained schedule for each vehicle is close to the optimal schedule with the same space and time complexity of linear insertion method. In this way, the batch-based method can be more efficient in large-scale ridesharing problem.

Table 2: Symbols and Descriptions.

Symbol	Description
R	a set of m time-constrained rider requests
r_i	ride request r_i of rider i
s_i	the source location of ride request r_i
e_i	the destination location of ride request r_i
c	the capacity constraint of a vehicle
G_i	a group of rider requests where $\lvert G_i \rvert \le c$
$\mathcal{P}$	a batch of requests in a time

To summarize, we make the following contributions in this paper:

- We introduce our STRide framework, which handles incoming requests in batch mode and adjusts the matching priority of requests in each batch in Section 2.3.
- We propose a graph structure called *shareability graph* for analyzing the sharing relationships between requests intuitively ridesharing problem, and designed an efficient algorithm to generate the shareability graph for each batch in Section 3.
- We devise a heuristic algorithm, namely *SARD*, for priority scheduling in each batch under the guidance of the shareability graph with theoretical analyses in Sections 4.
- We conduct extensive experiments on two real datasets to show the efficiency and effectiveness of our proposed STRide framework in Section 5.

In addition, the remaining sections of the paper are arranged as follows. We define the shareability graph and propose an efficient construction algorithm in Section 3. We review and compare previous studies on queuing theory and vehicle dispatching in Section 6 and conclude the work in Section 7.

2 PROBLEM DEFINITION

In this section, we introduce and analyze the batch-based dynamic ridesharing problem *BDRP* studied in this paper. Then, we introduce the overview of our STRide framework.

We use a graph $\langle V, E\rangle$ to indicate the road network, where V is a set of vertices and E is a set of edges between vertices. Each edge (u, v) is associated with a weight $cost(u, v)$ to represent the travel cost from u to v. In this paper, travel cost means the minimum travel time cost from u to v. When the speed is known, the minimum travel time cost can be directly transferred to the shortest travel distance.

2.1 Definitions

Definition 1 (Request)**.** Let $r_i = \langle s_i, e_i, n_i, t_i, d_i \rangle$ denote a ridesharing request with n_i riders from source s_i to destination e_i, which is released at time t_i and requires reach destination before delivery deadline d_i.

In online scenarios, each vehicle may be assigned with a certain number of requests. Therefore, we also need to plan a feasible schedule for each vehicle with allocated requests, which forms by the sequence of pickup and drop-off locations as definition 2 shows.

Definition 2 (Schedule)**.** Given a vehicle v_j with m allocated requests $R_j = \{r_1, \ldots, r_m\}$. Let $S_j = \langle o_1, \ldots, o_{2m} \rangle$ defines a schedule for v_j, where the location $o_x \in S$ is the source location or destination of a request $r_i \in R_j$.

We call the location o_i in schedule as a *way point*. A route S is *valid* if and only if it satisfies the following three constraints:

- **Order Constraint**. For any $r_i \in R_j$, the source location s_i appears before the destination e_i in the route S_j;
- **Capacity Constraint**. At any time, the total number of assigned riders must not exceed the maximum capacity c_j of vehicle v_j.
- **Deadline Constraint**. For any $o_x \in S$, the total driving time before o_x must satisfy the inequality 1.

$$\sum_{k=1}^{x} cost(o_{k-1}, o_k) \leq ddl(o_k). \tag{1}$$

Here, $ddl(o_k)$ is the deadline d_i when o_k is the destination of r_i, while $ddl(o_k) = d_i - cost(s_i, e_i)$ when o_k is the source of r.

To complete the arranged schedule on time, the vehicle has a maximum allowed detour distance at each way point. We define the maximum allowed detour time as *buffer time* in Definition 3.

Definition 3 (Buffer Time [15, 44])**.** Given a valid vehicle schedule $S_i = \langle o_1, o_2, \ldots, o_{2m} \rangle$, let $buf(o_x)$ be the maximum detour time at the way point o_x without violating the deadline constraints of its consequent way points.

$$buf(o_x) = \min \{buf(o_{x+1}), ddl(o_{x+1}) - arrive(o_{x+1})\}, \tag{2}$$

where $arrive(o_{x+1})$ is the earliest arriving time of way point o_{x+1} without any detour in previous way points in schedule S_i.

With the buffer time of each way point, we can find a suitable pickup and drop-off time for the new coming request in $O(n)$ time [44].

Based on these definitions above, *RTV-Graph* is proposed in [5] to describe the shareable relationship between requests and vehicles. The solution proposed for the dynamic ridesharing problem which based on RTV graph and linear programming in [5] could get a better result with the shorter total distance and higher service rate. However, in the process of constructing RTV graph, it needs to check whether any two or more requests can be shared with $O(n^c)$ time, and check whether each car can serve all requests in each trip in $O(m|T|)$ time. Therefore, it's not efficient enough to be used in a large-scale real application. In this paper, we proposed a simpler shareability graph for analyzing the shareable relationships instinctively to help solve dynamic ridesharing problem defined as following.

Definition 4 (Dynamic Ridesharing Problem)**.** Given a set, R, of n dynamically arriving requests and a set, V, of m vehicles. The goal of *Dynamic Ridesharing Problem* is to plan a feasible schedule for each vehicle $v_i \in V$, which minimized a specific utility function.

In *Batched Dynamic Ridesharing Problem* (BDRP), we need to resolve the problem in batch mode, which handles a few incoming requests in time period T as a batch $\mathcal{P}$ and then partitions into request groups $\mathbb{G} = \{G_1, G_2, \ldots, G_z\}$, which satisfied following conditions: $\forall G_x, G_y \in \mathbb{G}, G_x \cap G_y = \emptyset$ and $\mathcal{P} = \bigcup_{a=1..z} G_a$. Then we try to assign request groups for each vehicle while minimizing the utility function. In this work, we refer to the unified cost function UC in [44] and defined the following utility function U:

$$U(V, \mathcal{P}) = \alpha \sum_{v_i \in V} \mu(v_i, G_{v_i}) + \sum_{G_i \in G^-} p_i \tag{3}$$

$$\mu(v_i, G_{v_i}) = \sum_{x=1}^{|S_{v_i}|-1} cost(o_x, o_{x+1}), \tag{4}$$

where S_{v_i} is the planned schedule for vehicle v_i. And G^- is composed of the request groups which have not been assigned in each batch with a penalty p_i. In this paper, we define $p_i = \beta \sum_{r \in G_i} cost(r)$ with a parameter β. Note that, p_i can be modified to support other optimization goals.

Table 2 summarizes the commonly used symbols.

2.2 Hardness of Batched Dynamic Ridesharing Problem

Theorem 2.1 (Hardness of the BDRP). *The Batched Dynamic Ridesharing Problem defined in Definition 4 is NP-hard.*

PROOF. We prove the theorem by a reduction from the URR problem defined in [15], which has been proved to be a NP-hard problem. The URR problem can be brief described as following: Given a set R of m riders and a set V of n vehicles, each rider is associated with a source location s_i, destination location e_i, a pickup deadline rt_i^- and a drop-off deadline rt_i^+. The URR problem arranges riders to vehicles to maximize the utility function u with capacity constraint and time constraint.

For a given URR problem, we can transform it to an instance of BDRP problem: we partition the riders $r_i \in R$ into a single element set G_i, the route of G_i is a simple shortest path from s_i to e_i. In addition, we set the utility value for each vehicle and group pairs as $\mu'(v_j, G_{v_j}) = -\mu(v_j, r_i)$. Then, for this BDRP instance, we would like to arrange a request group for the given vehicle with a route such that the summation utility value $\sum_{v_j \in V} -\mu'(v_j, G_{v_j})$ is minimized. This shows that the URR problem can be solved if and only if the transformed BDRP can be solved.

In this way, we can reduce the URR problem to the BDRP. Since the URR problem has been proved to be NP-hard, BDRP is also NP-hard. This completes the proof of the theorem. □

Since BDRP is NP-hard, it is intractable. To efficiently and effectively solve BDRP, we propose a novel batch based framework, namely STRide, to exploit the structure information of shareability graph of requests to improve the performance of the dynamic ridesharing system on the service rate and total travel cost.

2.3 An Overview of STRide Framework

We first briefly introduce the major parts of our STRide framework, which is illustrated in Figure 2.

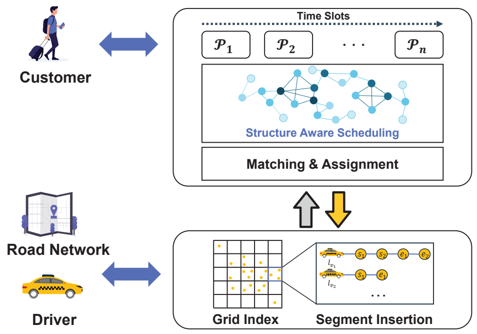

Figure 2: Overview of System Framework *STRide*.

Index Structure. In ridesharing, vehicles keep moving over time, which requires that the index we used must update efficiently. Grid index is an efficient index structure that can query and update moved vehicles in constant time (i.e., more efficient than many other spatial indexes such as tree-based indexes [34]). In STRide, we partition the road network into $n \times n$ square cells. With the grid index, we can retrieve all available vehicles efficiently through a range query for a given location p and a specified radius r in constant time.

Schedule Maintenance. In STRide, we need to arrange the pickup and drop-off locations of the new requests to the available vehicles' schedules. There are two wildly used solutions: *kinetic tree insertion* [25] and *linear insertion* [44, 50]. Kinetic tree insertion maintains all feasible schedules for a particular vehicle in a tree structure, and always returns the optimal schedule (i.e., the shortest total traveling cost). In contrast, the linear insertion method only maintain a current optimal schedule and inserts the way points into the maintained schedule in constant time without *reordering* way points, which means that it may miss the optimal schedule. However, Ma *et al.* [38] reveals that reordering way points almost has no change in effectiveness but needs more time and space. Therefore, we maintain the schedule for each vehicle by linear insertion.

Structure-Aware Assignment. We process the incoming requests into batches by their release timestamps and handle them in batch mode. For each batch, we utilize the shareability graph in Section 3 to analyze the sharing relationship between requests. In the *Matching and Assignment* phase, we proposed a two-phase algorithm SARD in Section 4, where the requests propose to valid vehicles in descending order of the additional travel cost (i.e., propose to vehicles needing more additional travel costs first), and vehicles select a group of structural friendly requests to accept. Here, we propose a novel measurement, namely shareability loss, to evaluate the harmfulness on merging a group of requests to a super node with respect to the sharing probability of the rest nodes in the shareability graph. The discarded requests will propose to other vehicles in the next proposal phase to improve the service rate.

3 SHAREABILITY GRAPH

Although the requests in a same batch have similar release times, the sharing probabilities of them can vary dramatically. For example, a request with a pair of popular source and destination has more opportunities to share a vehicle with other requests. Thus, an intuitive motivation for optimizing the grouping process is to associate higher priorities to the requests with lower shareability. Therefore, in this section, we proposed a *shareability graph* to manage the sharing relationships between requests with an efficient construction algorithm for it. With shareability graph, we can further analyze the shareability of requests in each batch.

3.1 Shareability Graph

Given a pair of requests r_a and r_b, we called r_a and r_b are *shareable* if there exist at least one feasible route for r_a and r_b to share.

Definition 5 (Shareability Graph)**.** Given a set of m requests R, let $SG = \langle R, E\rangle$ denotes a *shareability graph* with a set of nodes R and edges E, where each node in R indicates a request. Each edge $(r_a, r_b) \in E$ denotes r_a and r_b are shareable.

For example, in the *shareability graph* shown in Figure 1(b), the edge $e = (r_1, r_2)$ between r_1 and r_2 reflects that there exist one feasible route to serve them in a trip (e.g., a schedule of $\langle s_1, s_2, e_2, e_1\rangle$). With the shareability graph, we can easily find out the candidate shareable requests of each request by retrieving the neighbors in the shareability graph. Moreover, we have the following two observations with graph analysis techniques.

Observation 1. *The degree of each request in the shareability graph reveals its shareability and importance in the corresponding batch.* We can intuitively evaluate the sharing opportunities of requests through comparing their degrees in the shareability graph. We call the degree of a request as its *shareability*. For example, a request with a small shareability is often more urgent to select an appropriate shareable request; otherwise it will not share with any requests in the batch.

Observation 2. *The potential shareable requests tend to be denser in the shareability graph.* In graph databases, *Clique Detection* is a popular community detection problem, which shows the tight relationship between nodes in a graph [13, 40, 41]. In the shareability graph, by Theorem 3.1, if there exists a valid sharing schedule consists of k requests, there must exists a *k-clique* among the corresponding nodes. With this observation, we can prune some infeasible combinations in the grouping phase of each batch.

Theorem 3.1. *Let S be a valid sharing schedule for k requests, then the corresponding nodes of k requests in the shareability graph form a k-clique.*

PROOF. We prove it by contradiction. We have a set, R, of k requests, and there exist a valid sharing schedule S consisting of their sources and destinations. Assume the corresponding nodes of k requests in the shareability graph do not form a k-clique, which means there are at least two requests, $r_a, r_b \in R$, not connected.

Let S' be a subsequence of S through removing the sources and destinations of all other requests except for r_a and r_b. Removing the way points from S will reduce the detours, which will maintain the validation of S. Thus, S' must still be a valid schedule. According to the definition of shareability graph, there must be an edge connecting r_a and r_b in the corresponding shareability graph, which makes a contradiction with our assumption. In conclusion, the nodes of k requests forms a k-clique in the shareability graph. □

3.2 Ellipse and Angle Pruning Strategies

To build the shareability graph for each batch $\mathcal{P}_k$, the basic idea is to enumerate all pairs of requests (r_a, r_b) in $\mathcal{P}_k$ and check there exists a valid sharing schedule with linear insertion method. The number of times to call the shortest path query in such a process

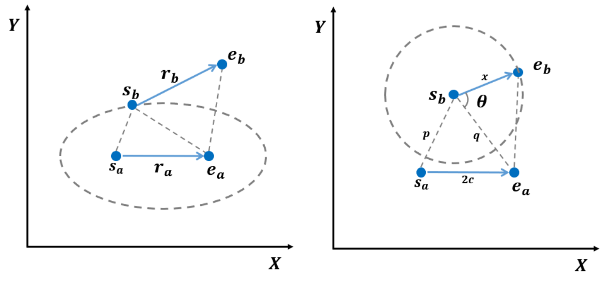

(a) Ellipse Pruning Example (b) Angle Pruning Example

Figure 3: A Illustration Example for *Shareability Graph Builder*

determines the efficiency of the construction algorithm. To avoid enumerating all pairs of requests, we propose two pruning strategies, ellipse pruning and angle pruning illustrated in Figure 3, for more efficient shareability graph construction. Note that, when we prune the candidates requests for a given request r_a, to avoid duplicated consideration of schedules, we only consider the schedules with s_a (the source of r_a) as the first way point.

Ellipse pruning. Our first pruning strategy is based on the source locations of the candidate requests, as we observe that the shareable requests share similar sources. If the sources of requests are far from each other, it's hard for drivers to deliver these requests on time in one trip due to the constraint of maximum waiting time. Therefore, for each request r_a, we prune the requests whose sources locating out the ellipse of r_a defined in Theorem 3.2 to avoid unnecessary shortest path query.

Theorem 3.2. *For a request r_a, the source s_b of its shareable request r_b must fall into the ellipse with s_a and e_a as the focus and $d_a/2$ as semi-major axis, where $cost(s_a, s_b) + cost(s_b, e_a) \le d_a$.*

PROOF. For any candidate shareable request r_b, there are only two feasible paths starting from s_a: (a) $\langle s_a, s_b, e_a, e_b\rangle$; (b) $\langle s_a, s_b, e_b, e_a\rangle$. The earliest arriving time of e_a is contributed by (a), which denoted as $arrive(e_a) = cost(s_a, s_b) + cost(s_b, e_a)$. Recall that r_a must be delivered to destination before deadline d_a, thus, $arrive(e_a) = cost(s_a, s_b) + cost(s_b, e_a) \le d_a$. This completes the proof. □

Angle pruning. Our second pruning strategy is based on the travel directions of the requests, as we notice that the requests with similar travel directions have a higher probability to share the trips. For instance, a northward request is hard to share with a southward request, because the driver needs to turn around and spend a lot of time to drive in the opposite direction to deliver the other passenger after finished one of them. We defined a threshold δ to prune request pairs that have similar sources but divergent directions with Theorem 3.3. Let $\overrightarrow{ab}$ be the vector pointing from a to b.

Theorem 3.3. *For a request r_a and its candidate sharing request r_b, the expected probability of successfully sharing a trip will increase when the angle θ between $\overrightarrow{s_b e_a}$ and $\overrightarrow{s_b e_b}$ decreases.*

PROOF. Firstly, we denoted the maximum detour time for request r_a as $(\alpha - 1) \times cost(s_a, e_a)$ where $\alpha \ge 1$. For the two possible schedules of r_a and its candidate request r_b ($\langle s_a, s_b, e_a, e_b\rangle$ or $\langle s_a, s_b, e_b, e_a\rangle$), one of the following two conditions needs to be satisfied due to the deadline constraint: (a) $p + x + cost(e_a, e_b) \le 2\alpha c$; (b)

Algorithm 1: *Shareability Graph* Builder

```
Input: A set $R$ of $n$ requests with an angle threshold $\delta$
Output: The corresponding shareability graph $SG$
1 $V = R$ and $E = \emptyset$
2 for $r_a \in R$ do
3     $C \leftarrow$ candidate requests filtered by Theorem 3.2
4     for $r_b \in C$ do
5         if $\arccos\left(\frac{\overrightarrow{s_b e_a} \cdot \overrightarrow{s_b e_b}}{|\overrightarrow{s_b e_a}||\overrightarrow{s_b e_b}|}\right) \in \left[-\frac{\delta}{2}, \frac{\delta}{2}\right]$ then
6             if $r_a$ and $r_b$ are shareable then
7                 $E = E \cup (r_a, r_b)$
8 return $SG = \langle V, E\rangle$
```

$p + q + cost(e_a, e_b) \le \alpha x$, where p, q, x and $2c$ indicate $cost(s_a, s_b)$, $cost(s_b, e_a)$, $cost(s_b, e_b)$ and $cost(s_a, e_a)$, respectively.

When request r_a, source s_b and $cost(s_b, e_b)$ are fixed, the total travel cost of the two possible schedules only depends on $cost(e_a, e_b)$. Then, $cost(e_a, e_b)$ can be represented through x, n and $\cos(\theta)$. In (a), we have $x \le \frac{(2\alpha c - p)^2 - q^2}{4\alpha c - 2p - 2q\cos(\theta)} \le 1/(\frac{cos^2(\theta/2)}{(\alpha+1)c} + \frac{sin^2(\theta/2)}{(\alpha-1)c})$ (noted as $g(c)$), because $p + q \le 2(\alpha + 1)c$ and $p - q \le 2(\alpha - 1)c$ hold in the ellipse in Theorem 3.2. In (b), we have $\alpha x \ge p + q + \sqrt{(x - q * cos(\theta))^2}$, which can be rewritten as $x \ge \frac{2c(1 - cos(\theta))}{\alpha - 1}$ (marked as $h(c)$) by $p + q \ge 2c$. It is worth noting that in both cases, with the decrease of the angle, the possible range of x increases gradually. In other words, for a given candidate request r_b, when the angle θ between $\overrightarrow{s_b e_a}$ and $\overrightarrow{s_b e_b}$ decreases, the travel cost $x = cost(s_b, e_b)$ is more likely to satisfy the deadline constraint. □

By investigating the real datasets of Chengdu and New York City in Section 5, we found that the distances of the requests almost follow the log-normal distribution whose probability density function is $f(x; \mu; \sigma) = \frac{1}{\sqrt{2\pi} x\sigma} e^{-\frac{(\ln x - \mu)^2}{2\sigma^2}}$, where μ and σ are two parameters of log-normal distribution. Therefore, the expected probability of r_a to share with a candidate request r_b with an angle θ is greater than a given threshold δ can be evaluated as follows:

$$\mathbb{E}(\theta \ge \delta) = \int_0^{+\infty} f(x)\left(\int_0^{g(\frac{x}{2})} f(y)dy + \int_{h(\frac{x}{2})}^{+\infty} f(y)dy\right)dx$$

For instance, we fit the probability density function of the requests' distances of Chengdu and NYC datasets with log-normal distribution. The probability expectations $\mathbb{E}(\theta \ge \frac{\pi}{2})$ are 40.98% and 41.38% respectively when $\alpha = 1.5$. Note that the requests we have ignored are either too short or hard to serve (i.e., long detour).

3.3 Shareability Graph Builder

The details of shareability graph builder algorithm is illustrated in Algorithm 1. Firstly, we initialize all requests as nodes in the shareability graph (line 1) and connect the shareable nodes gradually (lines 2-7). We try to find shareable relationship for each node successively (lines 2-7). With the benefit of Theorem 3.2, we can obtain a candidate request set C which shares a similar source location with r_a by the constant time calculation instead of the shortest path query. After that, we further identified the requests $r_b \in C$ by angle pruning rule (lines 4-7). We construct the vector $\overrightarrow{s, e}$ by the source and destination of the corresponding request to represent the distance and direction. If the angle θ of $\overrightarrow{s_b e_a}$ and $\overrightarrow{s_b e_b}$ is out of the given angle threshold δ, r_b will be pruned (line 5). We'll add an edge (r_a, r_b), if r_a and r_b are shareable (lines 6-7). Finally, we get a shareability graph *SG* composed of *V* and *E* generated in the above steps (line 8).

Complexity Analysis. Suppose that the shortest path query can be finished in $O(q)$. For a given request r_a, we can complete the filtering step within constant time by searching *Minimum Bounding Rectangle* of the ellipse in grid index. However, in the worst case, the size of $|C| = n - 1$ in line 3. In addition, the angle calculation can be also completed in constant time. We only need to perform two times insertion when testing whether r_a and r_b are shareable in $O(k)$. Thus, the final complexity of the algorithm is $O(q \cdot n^2)$.

4 STRUCTURE-AWARE DISPATCHING

With the shareability graph, we can intuitively analyze the shareability of each request and propose the structure-aware ridesharing dispatching (SARD) algorithm under the guidance of shareability graph. Specifically, we first discuss two main schedule maintenance methods in Section 4.1. Then we introduce a bottom-up enumeration strategy for different combination of requests in Section 4.2. Lastly, we elaborate the detail steps of SARD in Section 4.3.

4.1 Schedule Maintenance

There are two state-of-art strategies for schedule maintenance in previous work: kinetic tree insertion [25] and linear insertion [44, 50]. Kinetic tree maintains all feasible schedules and check all available way points ordering exhaustively to insert a new request. Even kinetic tree can get the *exact* optimal schedule for the vehicle, it needs to maintain up to $\frac{(2m)!}{2^m}$ schedules in the worst case (*m* is the number of requests assigned in vehicle). In contrast, the schedule obtained by linear insertion method is optimal only for the current schedule (i.e., local optimal). Linear insertion is optimal when the number of requests is 2. In the experimental study in Section 5, we find that in NYC and Chengdu datasets, if we use linear insertion to handle requests according to the release time of the request, the probability of achieving global optimal schedule is up to 89% and 85%, when we insert the third and forth request, respectively. To improve the probability of achieving global optimal schedule with the linear insertion method, we reorder the insertion sequence of the requests base on the Observation 1 in Section 3.1. Specifically, we first select two requests with the lowest shareability (i.e., the degree of node) in shareability graph and generate an optimal sub-schedule. Then, we insert the remaining requests into the sub-schedule one-by-one in the ascending order of their shareability. In this way, we improve the probability of achieving optimal schedule using linear insertion method up to 91% and 90%.

4.2 Request Grouping

In batch mode, we need to enumerate all feasible request combinations before the assignment phase. If we simply construct groups by enumerate all possible combinations, we need to check $\sum_{i=1}^{c} \binom{n}{i}$ groups, where *c* is the capacity of vehicles. For each group, we need to verify that whether there exists a feasible route to serve these requests in $O(k^2)$ by linear insertion [44], where *k* is the size of group. However, many groups are invalid for vehicles in practice. To avoid unnecessary enumeration, Zeng *et al.* propose an index called *additive tree* [53], which enumerates valid groups level by level through a tree-based structure. In additive tree, each node represents a valid group of requests, and the group for every node is an extension group from the group of its parent node through adding one more request.

Algorithm 2: Request Grouping Algorithm

```
Input: A shareability graph SG of a batch instance and a set R of n
       requests, the capacity of vehicles c
Output: Request groups set $\mathcal{RG}$.
1  initialize $\{RG_1, RG_2, \cdots, RG_c\}$ as empty sets
2  forall $r_a \in R$ do
3      $RG_1$.insert($\{r_a\}$, $\langle s_a, e_a \rangle$)
4  for $l \in [2..c]$ do
5      foreach pair $(G_x, G_y)$ in $RG_{l-1}$ do
6          $G \leftarrow G_x \cup G_y$
7          if $|G| = l$ and $G$ satisfied Lemma 4.1 then
8              $r_b \leftarrow$ find maximum degree node in $SG$
9              $S \leftarrow$ insert $r_b$ into the schedule $S'$ of $G \setminus \{r_b\}$
                 maintained in level $RG_{l-1}$
10             if $S'$ is valid then
11                 $RG_l$.insert$(G, S)$
12 return $\mathcal{RG} = \{RG_1, RG_2, \cdots, RG_c\}$
```

Although the additive tree can help to prune some invalid groups in the enumeration, it still needs to maintain all valid schedules for each node of the additive tree. However, we will only pick the best one of these schedules for each group at the end. With the schedule maintenance method proposed in Section 4.1, we can heuristically reorder the insertion sequence to get an optimal schedule with higher probability. Therefore, in building the modified additive tree, we only keep one schedule for each node by inserting one new request to its parent's schedule.

The detailed construction steps are shown in Algorithm 2. Firstly, we initialize *c* empty sets $\{RG_1, RG_2, \cdots, RG_c\}$ to store *c* levels of nodes for the modified additive tree (line 1). Then, we construct the groups formed by individual request $r_a \in R$ whose schedule is consisted of its source and destination for level 1 of the modified additive tree (line 2-3). For the construction of the feasible groups of the remaining levels RG_l, we generate each node in level *l* by traversing and merging pairs of parent nodes' groups RG_{l-1} (line 4-11). During constructing the nodes in level *l*, we only consider the groups *G* with *l* requests and *G* must satisfy Lemma 4.1 (line 7). For each feasible group *G*, we search for the request $r_b \in G$ with the maximum shareability in *SG* (line 8). Based on the schedule S' of its parent node for group $G \setminus \{r_b\}$, we generate the new schedule *S* of *G* through inserting r_b to S' with linear insertion method (line 9). If the generated schedule is valid for *G*, we store the new group with its maintained schedule (G, S) into RG_l (line 10-11).

Lemma 4.1. *For any valid group G_x: (a) $\forall r_a \in G_x$, the group $G_x \setminus \{r\}$ must be also valid; and (b) the nodes of $r_a \in G_x$ forms a clique in the shareability graph.*

PROOF. The first condition has been proved by Lemma 2 in [53] and condition (b) is derived from Theorem 3.1. □

Example 2. *Consider the example in Figure 1. We first initialize the groups composed of a single request with corresponding schedule. Then, we enumerate all pairs of 1-size groups and merge them to*

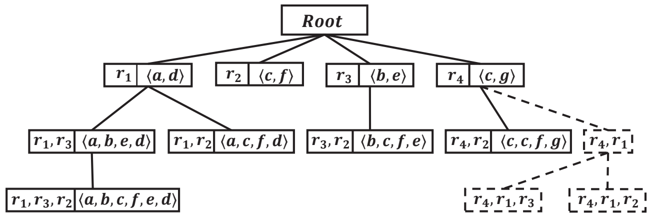

Root
r_1 $\langle a,d\rangle$
r_2 $\langle c,f\rangle$
r_3 $\langle b,e\rangle$
r_4 $\langle c,g\rangle$
r_1,r_3 $\langle a,b,e,d\rangle$
r_1,r_2 $\langle a,c,f,d\rangle$
r_3,r_2 $\langle b,c,f,e\rangle$
r_4,r_2 $\langle c,c,f,g\rangle$
r_4,r_1
r_1,r_3,r_2 $\langle a,b,c,f,e,d\rangle$
r_4,r_1,r_3
r_4,r_1,r_2

Figure 4: Grouping Tree in Example 2.

generate a new schedule for child nodes. Because $deg(r_2) > deg(r_3)$ in shareability graph SG in Figure 1(b), we maintain the schedule for group $\{r_3, r_2\}$ by inserting r_2 into the schedule of group $\{r_3\}$. The schedule generated by linear insertion method is optimal when the size of the group is 2. At the same time, we take the generated group $\{r_3, r_2\}$ as a child of group $\{r_3\}$. Since we cannot find a valid schedule for r_4, r_1, all groups containing $\{r_1, r_4\}$ are pruned in subsequent steps. Next, we insert r_2 into the schedule of group (r_1, r_3) and get an approximate schedule $\langle a, b, c, f, e, d\rangle$ because $deg(r_2) > deg(r_1) = deg(r_3)$. Since we cannot find any valid group G which $|G| \geq 4$, we terminate the group building process and got the final result as shown in Figure 4.

Complexity Analysis. In the worst case, all the requests in a batch can be arbitrarily combined, so that there are at most $\sum_{i=1}^{c}\binom{n}{i}$ nodes in total. Since the capacity constraint $c \ll n$ in practice, the number of combination groups can be noted as $O(n^c)$. For each new group, we only need $O(c)$ time to perform linear insert operation for a new schedule. We can finish the request grouping in $O(c \cdot n^c)$.

4.3 SARD Algorithm

With the grouping algorithm in Section 4.2, we proposed a two-phase matching algorithm, *SARD*, to solve the matching between vehicles and requests in this section. The intuition of SARD is to greedily maintain the shareability or connectivity of the nodes in the shareability graph such that the requests have higher rates to share with other requests in the final assignment and schedules. In SARD, requests at beginning propose to *worse* vehicles (with larger increases of travel costs), which can give more initiative to vehicles on selecting groups of requests. Then, for each vehicle v_j, it greedily accepts a group of proposed requests with the smallest *shareability loss*, and the rejected requests can propose to other better vehicles in the next round. The proposal and acceptance phases are iteratively conducted, until no request will propose. We first define shareability loss, then introduce two theorems to support our design of SARD.

To define shareability loss, we introduce a substitution operation to replace a k-clique G_i in shareability graph SG with a super node $\hat{v}_i$. After we substitute a super node $\hat{v}_i$ for a k-clique G_i, there is an edge connecting another node $v_j \in SG \setminus G_i$ with $\hat{v}_i$ if and only if v_j connects to every node of G_i in the original shareability graph. Then, we define shareability loss as:

Definition 6 (Shareability Loss)**.** Given a shareability graph $SG = \langle V, E\rangle$, the shareability loss $SLoss(G_i)$ of substituting a super-node $\hat{v}_i$ for a k-clique group $G_i \subseteq V$ is evaluated with the following structure-aware loss function:

$$SLoss(G_i) = \max_{r\in G}\{|\bigcap_{v\in G-\{r\}} N(v)| + |N(r)| - |\bigcap_{v\in G} N(v)| - 1\}, \quad (5)$$

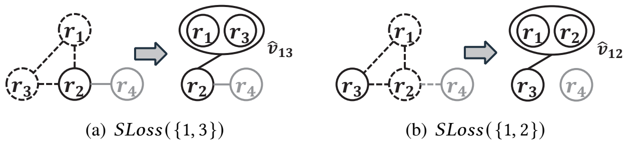

(a) $SLoss(\{1,3\})$ (b) $SLoss(\{1,2\})$

Figure 5: An Illustration Example of Shareability Loss

where $N(v)$ is the set of neighbor nodes of v in the shareability graph SG. $SLoss(G) = deg(r)$ if $|G| = |\{r\}| = 1$.

Example 3. *With the shareability graph in Figure 1(b), we illustrate the idea of shareability loss in Figure 5, where we assume r_4 is not available. In Figure 5(a), we try to merge r_1 and r_3 into a super node as follows. We first remove the edges incident to r_1 and r_3. Since r_1, r_2 and r_3 form a 3-clique in the original graph, there should be a shareable relation between r_2 and the super node $\hat{v}_{13} = \{r_1, r_3\}$ by Theorem 3.1. Thus, we add a new edge between r_2 and $\hat{v}_{13}$. Overall, if we substitute $\hat{v}_{13}$ for $\{r_1, r_3\}$, the shareability loss is $SLoss(\{r_1, r_3\}) = 3 - 1 = 2$. In Figure 5(b), we try to merge r_1 and r_2 into a super node $\hat{v}_{12} = \{r_1, r_2\}$. Similarly, four edges incident to r_1 and r_2 are removed, and a new edge between $\hat{v}_{12}$ and r_3 is built. Then, the shareability loss is $SLoss(\{r_1, r_2\}) = 4 - 1 = 3$ here. Therefore, substituting $\{r_1, r_3\}$ is more structure-friendly than substituting $\{r_1, r_2\}$.*

Shareability loss can guide a vehicle to select a set of requests to serve from the potential requests (i.e., proposed to the vehicle in the proposal phase). Specifically, a vehicle v_j should select a set of requests whose shareability loss is the minimum among all groups of its potential requests. In Theorem 4.1, we prove that through serving a group of requests with the smallest shareability loss, the remaining requests can have higher upper bound of sharing rate.

Theorem 4.1. *Substituting a super-node for group G with smaller shareability loss will increase the upper bound of sharing probabilities more for the remaining nodes in the shareability graph.*

PROOF. According to Theorem 3.1, all valid groups we picked in the assignment phase always constitute a k-clique in the shareability graph. Therefore, we model the problem of maximizing sharing probability as a problem of clique partition [30], which trying to find the minimum number of cliques to cover the graph such that each node appear in exactly one clique. In the worst case, we will partition each node in the shareability graph into a 1-clique, and then the sharing probability of the nodes is 0 (i.e., no requests can share with each other). Intuitively, the less clique we used to cover the shareability graph, the higher the sharing probability is. Thus, we transform our problem into clique partition. Moreover, because of the capacity constraint k to each feasible group in our problem, we consider the problem of partitioning the shareability graph into minimum number of cliques which size is not larger than k. In [9], J. Bhasker *et al.* present an optimal upper bound (shown in equation 6) for the clique partition problem evaluated with the number of nodes n and the number of edges e for the graph.

$$\theta_{upper} = \lfloor \frac{1 + \sqrt{4n^2 - 4n - 8e + 1}}{2} \rfloor \quad (6)$$

In addition, we observed that the degrees of most riders in the shareability graph are relatively small, in line with the characteristics of power-law distribution. For analytical tractability, we assume that the degree of the node in the shareability graph as a random variable δ following the power-law distribution with exponent α,

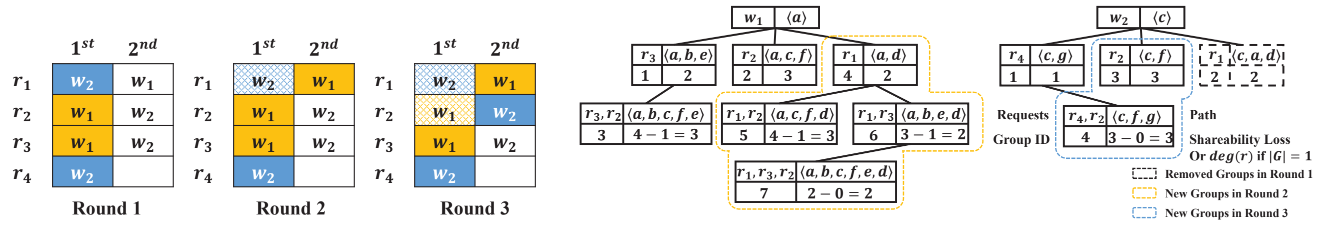

(a) Transformation of the Candidate Queue

(b) Grouping Trees for Vehicles

Figure 6: An Example for the *SARD* Algorithm

which complementary cumulative distribution shown as $\Pr(\delta \geq x) = ax^{-\alpha}$. For a shareability graph SG having n nodes and the degree of its each node follows the power-low distribution with exponent α, Janson *et al.* [28] reveal that the size of the largest clique $\omega(SG(n,\alpha))$ in graph SG is a constant with $\alpha > 2$. However, in the heavy-tail distribution, $\omega(SG(n,\alpha))$ grows with $n^{1-\alpha/2}$ (the formal description is shown in equation 7).

$$\omega(SG(n,\alpha)) = \begin{cases} (c + o_p(1))n^{1-\alpha/2}(\log n)^{-\alpha/2}, & \text{if } 0 < \alpha < 2 \\ O_p(1), & \text{if } \alpha = 2 \\ 2 \text{ or } 3 \text{ w.h.p}, & \text{if } \alpha > 2 \end{cases} \tag{7}$$

For any shareability graph SG, we deal with the optimal partition $\{C_1 \ldots, C_\theta\}$ of general clique partition problem on SG as follows: for each clique C_i, we divided C_i into sub-cliques with size no larger than k. After that, we obtained an upper bound θ'_{upper} after scaling of our problem with n and e by formula 6 and 7.

$$\theta'_{upper} = \lfloor \frac{1 + \sqrt{4n^2 - 4n - 8e + 1}}{2} \rfloor \cdot \lceil \frac{\omega(SG(n,\alpha))}{k} \rceil \tag{8}$$

The higher the number of edges e in the shareability graph SG is, the lower the upper bound θ'_{upper} of the number of clique partitions is. In conclusion, substituting a super node for the group of nodes with the lowest edge loss will keep the most number of edges left in the shareability graph SG, which improves the sharing probabilities of the remaining nodes in SG. This completes the proof. □

To merge nodes whose degree are 2 in the shareability graph at the beginning, we have the following theorem:

Theorem 4.2. *Given a shareability graph $SG = (V, E)$, merging the node v, whose degree is 1, with its neighbor into a 2-clique will not reduce the pairing rate in SG.*

PROOF. Suppose that the minimum clique partitions with size no larger than k on SG are $\{C_1, \ldots, C_n\}$, and v_x and v_y are included in C_a and C_b, respectively. The size of the clique $|C_a| \leq 2$ because $deg(v_x) = 1$. If v_x and v_y are included in different partitions ($a \neq b$), the size of the clique $|C_a| = 1$ because v_x is not connected to any node except v_y. Thus, removing v_y from C_b and merging it into C_a will not increase the number of isolated groups, whose sizes are not larger than 1. Otherwise, ($a = b$), v_x and v_y are included in the same partition and forms a 2-clique, which is consistent with the theorem. Thus, the operation in the theorem will not violate the pairing rate of nodes on SG. This completes the proof. □

With Theorems 4.1 and 4.2, we design our SARD, whose pseudo code is shown in Algorithm 3. Firstly, we maintain a current working set R_p (line 1), which contains all available requests until the current

Algorithm 3: *SARD*

```
Input: A set $R$ of $n$ requests with a batching time period $T$ and a set
       $W$ of $m$ vehicles
Output: A vehicle set $W$ with updated schedules.
1  $W \leftarrow$ initialize a working set for unmatched and unexpired requests
2  foreach batch $\mathcal{P}$ within time period $T$ do
3      insert $r_a \in \mathcal{P}$ into working pool $R_p$
4      $SG \leftarrow$ build shareability graph for $W$ with Algorithm 1
5      foreach $r_a \in R_p$ do
6          $Q_{r_a} \leftarrow$ initialize a priority queue by $\Delta$ utility
7          insert candidate vehicles into $Q_{r_a}$
8      while $\exists r_a \in R_p, |Q_{r_a}| \neq 0$ do
9          foreach $r_a \in R_p$ and $|Q_{r_a}| \neq 0$ do          ▷ Proposal Phase
10             $w_x \leftarrow Q_{r_a}$.pop() the worst vehicle
11             $R_{w_x}$.insert($r_a$)
12         foreach $w_x \in W$ do                                   ▷ Acceptance Phase
13             $G_{w_x} \leftarrow$ grouping $R_{w_x}$ by Algorithm 2
14             $G^*_{w_x} \leftarrow$ select a group with minimum shareability loss
                from $G_{w_x}$
15             push $w_x.ac \setminus G^*_{w_x}$ back to $R_p$ for next proposal
16             foreach $r_b \in G^*_w$ do
17                 remove $r_b$ from $R_{w_x}$ and add $r_b$ to $w_x.ac$
18     remove expired requests from $R_p$
19     return $W$
```

timestamps. When each batch arrives, we insert the requests in this batch R_p (line 3) and process them together with the available (unmatched and unexpired) request in the previous round (lines 2-18). Before starting the two-phase processing, we retrieve all candidate vehicles for each request r_a and store them into a priority queue Q_{r_a} in descending order of the increased utility cost for serving r_a (lines 5-7). In the proposal phase (lines 9-11), each request which has not been accepted in the previous round will propose to its current worst vehicle (i.e., the vehicle with the largest travel cost increase on serving the request) (line 11). After that, we enumerate the feasible groups of requests received by each vehicle w_x by Algorithm 1. We evaluate the validation of group nodes based on w_x's current schedule (line 13). Specifically, we replace the single request schedule in the line 3 of Algorithm 1 with the schedule generated by inserting the request into the worker's current schedule, which helps to filter out the groups that cannot be served by vehicle w_x. With Theorem 4.1, we prioritize the groups with a smaller shareability loss. We select a set of group with the minimum shareability loss for vehicle w_x(line 14). Then, we put the discarded requests back to working pool R_p (line 15), where $w_x.ac$ indicates the current accepted requests of

Table 3: Experimental Settings.

Parameters	Values
the number, n, of requests	10K, 50K, 100K, 150K, 200K, **250K**
the number, m, of vehicles	1K, 2K, 3K, 4K, **5K**
the capacity of vehicles c	2, 3, **4**, 5, 6
the deadline parameter γ	0.2, 0.3, **0.5**, 0.8, 1.0
the penalty coefficient p_r	2, 5, **10**, 20, 30
the batching time Δ (s)	1, 3, **5**, 7, 9

vehicle w_x. At the end of each acceptance phase, we assign the selected group to the vehicle and put the rejected and evicted requests back into the working set R_p for their subsequent proposal (lines 16-17). We repeat the proposal and acceptance phase until no request will propose. Finally, we remove the expired requests from R_p that cannot be completed due to exceeding the maximum waiting time at the end of each batch.

Example 4. *Let's consider the batch of requests in Example 1. Suppose there are two idle vehicles, w_1 and w_2, located at a and c. We first construct a candidate vehicle queue for $r_1 \sim r_4$. For instance, the travel cost of w_1 and w_2 for serving r_1 is $cost(r_1)$ and $cost(r_1) + cost(c, a)$, respectively. The priority sequence in r_1's candidate queue is $\langle w_2, w_1 \rangle$. In this way, we can calculate the candidate queue of the remaining requests, as shown in the Figure 6(a). In the first round, r_2 and r_3 are put into the candidate pool of w_1, while the remaining requests are put into the candidate pool of w_2. Then, w_1 and w_2 enumerate all the groups by Algorithm 2 with the requests in their candidate pool (as shown in Figure 6(b), except for the colored dashed area). In the grouping of w_1, we take $\{r_3, r_2\}$ as the temporal assignment because it's the only group whose size is not less than 2. Since there are no groups whose size is not less than 2 in the first round of w_2, we prefer the group $\{r_4\}$ which has lower degree by default as it leads to less shareability loss. Since r_1 is not accepted by vehicle w_2, it will propose to w_1 according to its candidate list in the second round. At this time, the w_1's grouping tree will be updated to the groups shown in the Figure 6(b). Although the loss of G_6 and G_7 are same, w_1 will update its current best group to $\{r_1, r_3\}$ rather than $\{r_1, r_3, r_2\}$, because the planned route of G_6 holds higher sharing ratio $\frac{cost(P)}{\sum_{r \in SG} cost(r)}$. Therefore, r_2 will be discorded and propose in the third round, and w_2 will take $\{r_4, r_2\}$ by Theorem 4.2. Finally, w_1 and w_2 was assigned with $\{r_1, r_3\}$ and $\{r_2, r_4\}$, respectively.*

Complexity Analysis. With grid index, we can retrieve the candidate vehicles in a constant time for each request. We need to perform an insertion operation in $O(c)$ time to obtain the increased travel cost. Thus, the time cost of constructing candidate queues for a batch of size n is $O(c \cdot n^2)$. In proposal phase, every request will propose to every car at most one time in the worst case. Thus, we need to build a grouping tree of the whole batch for each car in $O(m \cdot n^c)$. The time complexity of *SARD* is $O(c \cdot n^2 + m \cdot n^c)$ in total.

5 EXPERIMENTAL STUDY

5.1 Data Set

The road networks of *CHD* and *NYC* are retrieved as undirected graphs. The nodes in the graph are intersections, and the edges' weight represents the required travel time on average. The shortest path query on the road network adopts the hub labeling algorithm [33] with LRU cache [26] for all algorithms. The details of the road networks are shown in Table 4.

Table 4: Details of Road Networks.

Name	#Nodes	#Edges	#Requests
CHD	214,440	466,330	259,347
NYC	112,572	300,435	424,635

We conduct experiments on two real datasets [44]. The first dataset is the requests collected by Didi in Chengdu, China (noted as *CHD*). The second one is the yellow and green taxi in New York, USA (noted as *NYC*). These datasets contain the following information about the request: release time, longitude and latitude of the source location and destination, and the number of passengers. We extracted the requests of the day with the largest number of requests as our request data (November 18, 2016 and April 09, 2016). We set the deadline of request r_i as $d_i = t_i + (1 + \gamma) * cost(r_i)$, which is a commonly used configuration method in many existing works [14, 26, 46]. In practice, the waiting time accepted by the request is limited. Therefore, we set the maximum waiting time threshold for requests to be 5 minutes, which means $w_i = \min(5min, d_i - cost(r_i) - t_i)$. The distribution of the sources and destinations of the datasets are shown in Figure 9. The source and destination of the requests are mapped to the corresponding node of the road network in advance. The initial position of the vehicle is randomly selected from the road network. The number of vehicles changes according to the experimental settings. In addition, we set all vehicles to have the same capacity c. In the following experiments, we use CHD's data for a whole day and NYC for half a day (with about 250k requests for each dataset). Table 3 shows the parameter settings, and default values are in bold.

5.2 Approaches and Measurements

We compare our algorithm with the following algorithms:

- ***pruneGDP [44].*** It inserts the request into the vehicle's current schedule sequentially and selects the vehicle with the least increased distance for service.
- ***RTV [5].*** It processes the requests in batch mode and obtains an allocation scheme with the least increased distance and the most number of serving vehicles by linear programming.
- ***GAS [53].*** It divides requests into batches and enumerates all combinations for each vehicle's candidate requests in random order. Then, it selects the most profitable group for each vehicle. The lengths of all requests in the group are used as the profit.
- ***RAND.*** It randomly arranges requests to a feasible vehicle sequentially, and the trip schedule of the vehicle is maintained by the linear insertion method [44].

We report the unified cost, service rate and overall response time of all algorithms. Specifically, the unified cost adopts the evaluation of total revenue in [44], and the varying penalty coefficient p_r is equivalent to the balance between income per unit time and fare per unit distance. We conduct experiments on a single server with Intel Xeon 4210R@2.40GHz CPU and 128 GB memory. All the algorithms are implemented in C++ and optimized by -O3 parameter. Besides, we use *glpk* [1] to solve the linear programming in *RTV* algorithm and all algorithms are implemented in single thread.

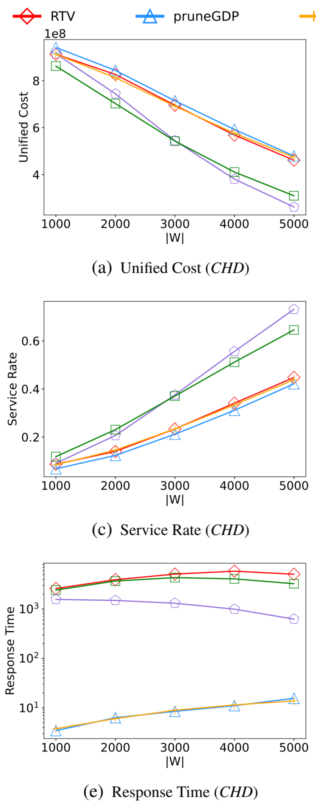

(a) Unified Cost (*CHD*) (b) Unified Cost (*NYC*)

(c) Service Rate (*CHD*) (d) Service Rate (*NYC*)

(e) Response Time (*CHD*) (f) Response Time (*NYC*)

Figure 7: Performance of varying $|W|$.

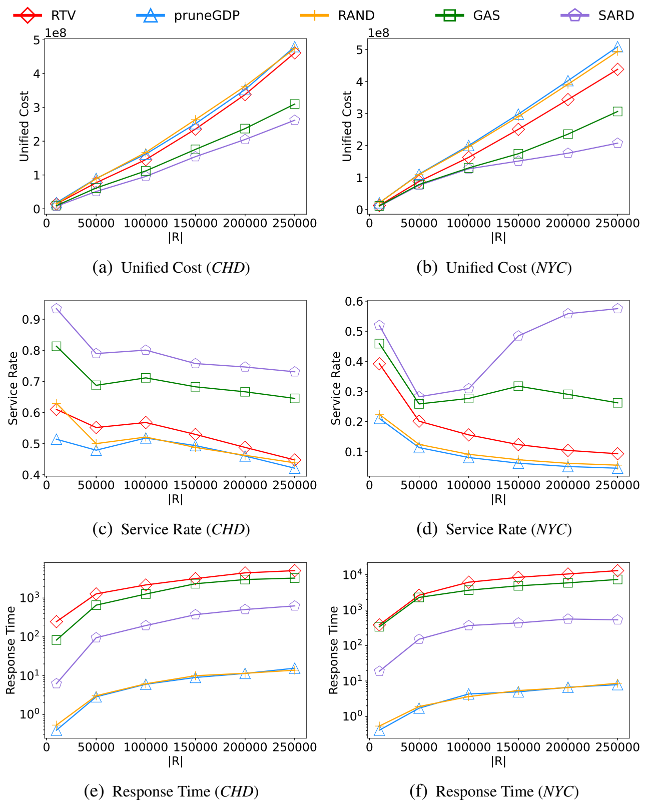

(a) Unified Cost (*CHD*) (b) Unified Cost (*NYC*)

(c) Service Rate (*CHD*) (d) Service Rate (*NYC*)

(e) Response Time (*CHD*) (f) Response Time (*NYC*)

Figure 8: Performance of varying $|R|$.

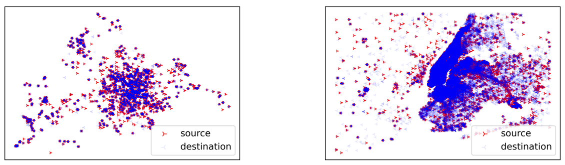

(a) Requests distribution (*CHD*) (b) Requests distribution (*NYC*)

Figure 9: The distribution of datasets.

5.3 Experimental Results

Effect of the number of vehicles. Figure 7 shows the results of varying the number of vehicles from 1K to 5K. With the increasing number of vehicles, all the results are getting better. In terms of unified cost, SARD and GAS are ahead of other methods, and the gap between these two algorithms and other algorithms is gradually widening. In the *CHD* dataset, the results of the two algorithms are very close, but SARD achieves an improvement of 2.09% $\sim$ 59.22% compared with other methods in the *NYC* dataset. As for serve rate, since the penalty part of the unified cost caused by the rejected requests decreasing when the algorithm achieves a higher overall service rate, the gap between the algorithms is consistent with the trend of unified cost. Compared with other existing methods, our method can obtain an improvement on service rate up to 30.99% and 52.99% on two datasets, respectively. pruneGDP and RAND are the winners in terms of the response time due to the efficiency of linear insertion. RTV, GAS and SARD are slower than pruneGDP. Specifically, SARD achieves a speedup ratio up to 7.12× and 23.5× than RTV and GAS on two datasets, respectively.

Effect of the number of requests. Figure 8 presents the results of varying the number of requests from 10K to 250K. Because the number of accepted and rejected requests increased significantly with the increase of requests number, the unified costs of all experiment algorithms are growing. Meanwhile, SARD and GAS achieve smaller unified costs than other methods when the number of requests becomes larger. For service rate, SARD improves the service rate by 41.97% $\sim$ 52.99% at most compared with pruneGDP. Besides, compared with the state-of-art batch-based method GAS, SARD can achieve up to 12.09% and 31.27% higher serve rates on the two datasets, respectively. For response time, the insertion-based methods are still faster. But among the batch-based methods (i.e., SARD, RTV and GAS), SARD is 4.21× $\sim$ 38.6× faster than GAS and RTV on two datasets.

Effect of deadline. Figure 10 presents the results of varying deadline of requests by changing the deadline parameter γ from 0.2 to 1. For service rate, the results of SARD is similar to the existing algorithms when we set the deadline of requests strictly, i.e., $\gamma = 0.2$. The reason is that the candidate vehicles for each request are greatly reduced with a minor deadline, then it is difficult to apply the grouping strategy in batch mode to improve the performance significantly. With the increase of deadline, the superiority of SARD and GAS gradually realizes. The service rate of SARD is more than 90% when the deadline is 1.8×, which is up to 37.42% higher than other existing algorithms on *CHD* dataset. The superiority of SARD is more explicit in the *NYC* dataset, where the service rate of SARD is up to 83.98% higher than that of pruneGDP. GAS performs inefficient on *NYC* dataset with $\gamma = 2.0$, which is mainly caused by increasing of the number of

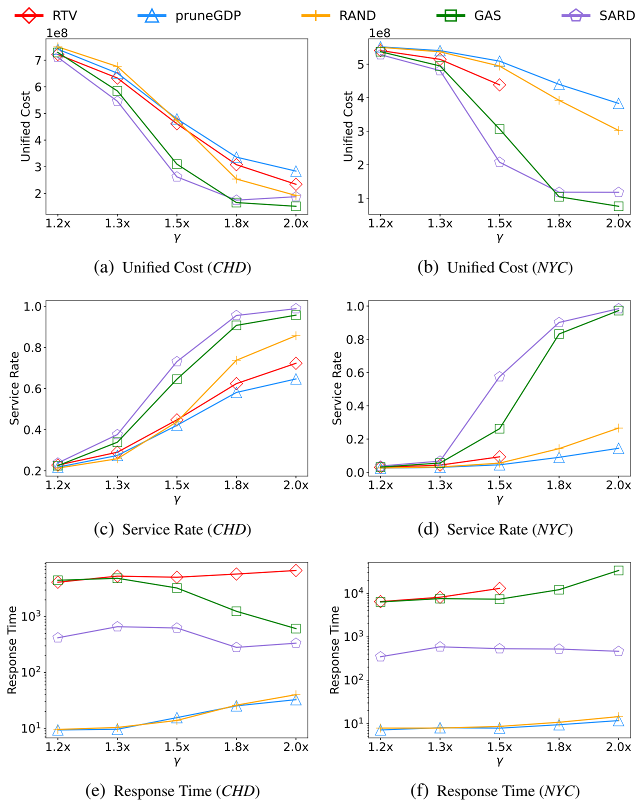

(a) Unified Cost (*CHD*) (b) Unified Cost (*NYC*) (c) Service Rate (*CHD*) (d) Service Rate (*NYC*) (e) Response Time (*CHD*) (f) Response Time (*NYC*)

Figure 10: Performance of varying γ.

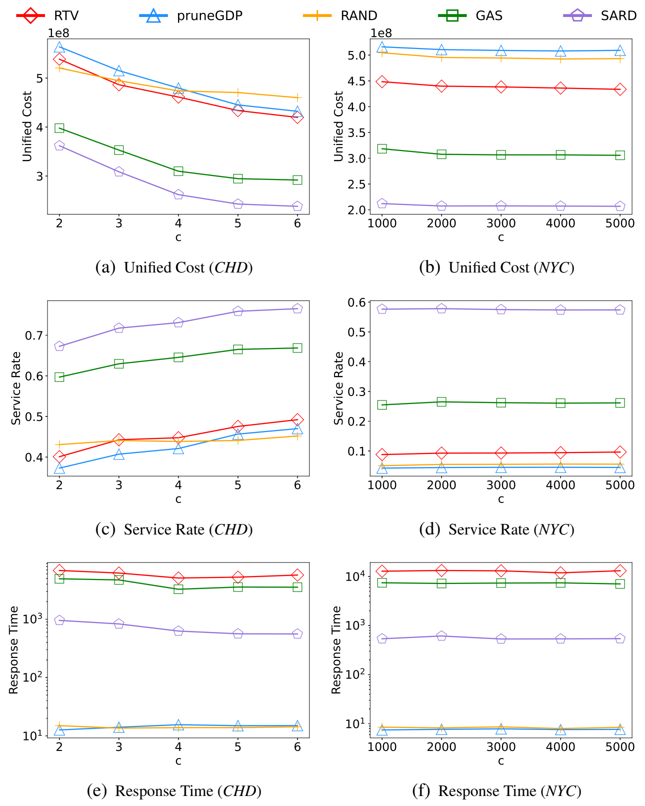

(a) Unified Cost (*CHD*) (b) Unified Cost (*NYC*) (c) Service Rate (*CHD*) (d) Service Rate (*NYC*) (e) Response Time (*CHD*) (f) Response Time (*NYC*)

Figure 11: Performance of varying c_r.

Table 5: Performance of Pruning Strategies.

Method	**City**	**Unified Cost**	**Service Rate**	**#Shortest Path Queries**	**Time (s)**
SARD	*CHD*	263,682K	72.82%	2,971,425K	699.8
	NYC	206,754K	57.64%	1,373,047K	770.6
SARD-O1	*CHD*	260,641K	73.34%	2,839,734K	662.0
	NYC	206,470K	57.83%	1,270,116K	750.6
SARD-O2	*CHD*	261,969K	73.10%	2,687,618K	626.9
	NYC	207,594K	57.50%	1,012,272K	595.1

request combinations with the relaxation of the deadline. Besides, GAS enumerates all the combinations of requests and schedules almost for each vehicle. The number of candidate requests increases as the number of requests increases. However, in SARD, the requests are proposed to different vehicles in a more decentralized way in each round, and the requests only go to the next round of enumeration after being discarded. Thus, the time cost for the combination enumeration of each vehicle is greatly reduced in SARD benefiting from our "proposal-acceptance" execution strategy. The results of RTV in *NYC* dataset with $\gamma \geq 1.8$ are not presented because the constraints of RTV-Graph exceeds the limit of *glpk* [1]. Meanwhile, SARD performs the best in terms of unified cost, which saves up to 48.03% and 73.16% compared with other existing algorithms on two datasets. For the response time, RAND and pruneGDP are the fastest, while SARD is the runner-up. SARD is 1.83× ∼ 72.68× faster than RTV and GAS.

Effect of vehicle's capacity constraint. Figure 11 illustrates the results of varying the vehicle's capacity from 2 to 6. In terms of unified cost, SARD and GAS save at least 30.87% compared with other tested algorithms. The unified cost of RAND is slightly better than that of pruneGDP in the case of smaller capacity. However, with the increase of vehicle capacity, pruneGDP gradually performs better than RAND on *CHD* dataset. This is because the increase of vehicle capacity will not affect the process of random selection of vehicles, which has not considered the different increased cost for each vehicle. On the contrary, pruneGDP will greedily choose the vehicles with the least increased distance for service, thus pruneGDP achieves a better result with large capacity than RAND. For a similar reason, the increase of vehicle capacity affects the number of edges between vehicles and trips in RTV-Graph, thus RTV shares a similar trend with *pruneGDP* in Fig 11(a). As for service rate, SARD still is the best among all tested algorithms (7.58% ∼ 53.39% higher service rate than other tested algorithms). In terms of response time, SARD still is the fastest in batch-based methods (RTV, GAS and SARD), which is 5.17× ∼ 17.52× faster than RTV and GAS.

Due to space limitation, please refer to Appendix A of our technical report [4] for the results and discussion about the experiments on varying penalty coefficient p_r and the batching time Δ.

Effects of pruning strategies. Table 5 shows the effect of the Ellipse and Angle pruning strategies proposed in Section 3.2 (parameters are in default values in Table 3). We note the method without pruning strategies as *SARD*, with the Angle pruning as *SARD-O1*, with Angle and Ellipse pruning as *SARD-O2*. The effect of pruning strategies of SARD-O2 save 9.55% and 26.28% of the shortest path queries and save 10.42% and 22.77% of the total running time on the two datasets compared with SARD, respectively. Besides, it has no noticeable harm on the service rate and unified cost.

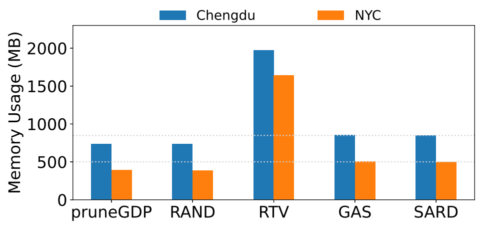

Figure 12: Memory Consumption.

Memory consumption. Figure 12 shows the memory usage of tested algorithms under the default parameters. The online mode algorithms follow the first-come-first-serve mode and use the less memory. In contrast, the batch mode algorithms need additional storage to store the combinations of requests in each batch (e.g., RTV-Graph for RTV, additive index for GAS, shareability graph for SARD). Since RTV rely on an integer linear program, the memory usage in RTV is more than twice of that in GAS and SARD. In addition, the cost of storing an undirected and unweighted shareability graph is close to each other in SARD and GAS.

Discussion. (1) *Running Time*. The complexity of online methods, pruneGDP and RAND, is $O(n^2)$, and thus they are the fastest in the experiments. RTV, GAS, and our SARD are batch-based algorithms. The time complexity of RTV is $O((m|G|)^c)$, where m is the number of vehicles, $|G|$ is the number of possible combinations of n tasks in the batch and can be notated as n^c. The time complexity of GAS is $O(T_s + mT_c)$, where T_s is the complexity of building additive index (as $O(n^c)$), and T_c is the time complexity of greedily searching the additive index (as O(n^c)). Our SARD needs $O(cn^2 + mn^c)$, where m and n are the numbers of vehicles and requests, respectively. For simplicity, we can note the time complexities of RTV, GAS and SARD as $O(m^c n^2 c)$, $O(mn^c)$ and $O(mn^c)$, respectively. GAS and SARD are faster than RTV. Different from GAS, our SARD only enumerates combinations among the proposed requests for each vehicle, thus n in SARD is much smaller than that in GAS. Although SARD has multiple rounds of propose-acceptance, due to the small n, it is still much faster than GAS. (2) *DataSet*. In the *NYC* dataset, the number of requests per unit time is about twice that of *CHD*. It means that in a same batch time, the algorithms based on the combination enumeration strategy (i.e., SARD and GAS) can obtain more candidate schedules, thus perform better in *NYC* than *CHD*. In addition, *NYC*'s road network is more compact than *CHD* (the nodes are only half of *CHD*), and the requests are more concentrated. Therefore, the requests in *NYC* have higher chances to share with each other in NYC. Thus, SARD performs better in *NYC* than *CHD* in most experiments. (3) *Scalability*. For the scalability of SARD, multi-threading can speed up the building of the Shareability Graph and accelerate the acceptance stage since each vehicle makes its decision independently. In practice, our SARD can be implemented with streaming distribution computation engines (e.g., Apache Flink [10]) and apply a tumbling window strategy to extend to the distribution environment.

Summary of the experimental study:

- The batch-based methods (i.e., RTV, GAS and SARD) can get less unified costs and higher service rates than the online-based methods (i.e., pruneGDP and RAND). For instance, the service rate of SARD is up to 50% higher than that of other tested methods.
- SARD runs up to 72.68 times faster than the other batch-based methods, RTV and GAS. For example, in Figure 10(f), SARD can process *NYC* requests in 8 minutes, but GAS takes up to 9 hours.

6 RELATED WORK

With the development of GPS equipment, mobile Internet, and sharing economy, ridesharing service has gradually become an indispensable choice for people to travel. The ridesharing problem can be reduced to a variant of the Dial-a-Ride (DARP) problem [19, 48], which aims to plan the vehicle routes and trip schedules for n riders who specified source and destination with practical constraints. The existing works on ridesharing service can be classified into static or dynamic according to whether all user requests are known in advance. Most of the existing works [18, 49] on DARP are working in static environment. For the dynamic ridesharing problem, the existing solutions are mainly in online mode [25, 37, 44, 50] or batch mode [5, 53, 55, 56]. In online mode, *insertion*[29] is the state-of-the-art operation of the existing works [23, 27] in route planning, which inserts the pickup and drop-off locations of the request into the vehicle's schedule without reordering. The insertion-based algorithms are more efficient in practice on real-life datasets [50]. Furthermore, in [44], Tong *et al.* proposed an improved insertion method based on dynamic programming, which checks the constraints in constant time and dispatches requests in linear time. On the other hand, Huang *et al.* proposed the structure of kinetic tree in [25], which is used to trace all feasible routes for each vehicle to reduce the total drive distance. With the kinetic tree, they always provide the optimal schedule for vehicles whenever the schedule changes (i.e., new rider arrives). For batch-based algorithms, they usually partition the request into groups with a schedule, and then assign groups to their appropriate vehicles. In [5], Alonso-Mora *et al.* propose RTV-Graph to model the relationship and constraints among requests, trips and vehicles, where trips are the groups composed of shareable requests. With the RTV-Graph, they minimize the utility function by linear programming to get the allocation result between vehicles and trips. But the time cost for enumerating trips in the process of building RTV-Graph grows exponentially. In [53], Zeng *et al.* proposed an index called additive tree for pruning the infeasible groups during the group enumeration, and greedily choose the most profitable request group to server for each vehicle. However, no existing work takes the priority of serving riders in the same batch into account. We proposed the structure of shareability graph and propose a two-phase heuristic algorithm, namely SARD, which exploits the structures to prioritize the requests in the assignment.

7 CONCLUSION

In this paper, we study the dynamic ridesharing problem with batch-based processing strategy. We first proposed a graph based shareability graph to reveal the sharing relationship between requests in each batch. With the structural information of the shareability graph, we measure the shareability loss of each request group. Furthermore, we devised a heuristic algorithm *SARD*, which adopts a two-phase strategy of "proposal-acceptance". In the experiments, the results on real datasets demonstrated that our method achieves better service rate, less unified cost with less running time compared with the state-of-the-art batch-based methods [5, 53].

REFERENCES

[1] 2016. [Online] GNU GLPK . https://www.gnu.org/software/glpk/.

[2] 2018. [Online] Didi Chuxing . https://www.didiglobal.com/.

[3] 2018. [Online] uberPOOL . https://www.uber.com/.

[4] 2021. [Online] Technical Report . https://cspcheng.github.io/pdf/ShareGraphRidesharing-Report.pdf.

[5] Javier Alonso-Mora, Samitha Samaranayake, Alex Wallar, Emilio Frazzoli, and Daniela Rus. 2017. On-demand high-capacity ride-sharing via dynamic trip-vehicle assignment. *Proc. Natl. Acad. Sci. USA* 114, 3 (2017), 462–467.

[6] Mohammad Asghari, Dingxiong Deng, Cyrus Shahabi, Ugur Demiryurek, and Yaguang Li. 2016. Price-aware real-time ride-sharing at scale: an auction-based approach. In *Proceedings of the 24th ACM SIGSPATIAL International Conference on Advances in Geographic Information Systems, GIS 2016*. 3:1–3:10.

[7] Mohammad Asghari and Cyrus Shahabi. 2017. An On-line Truthful and Individually Rational Pricing Mechanism for Ride-sharing. In *Proceedings of the 25th ACM SIGSPATIAL International Conference on Advances in Geographic Information Systems, GIS 2017, Redondo Beach, CA, USA, November 7-10, 2017*. 7:1–7:10.

[8] Xiaohui Bei and Shengyu Zhang. 2018. Algorithms for Trip-Vehicle Assignment in Ride-Sharing. In *Proceedings of the Thirty-Second AAAI Conference on Artificial Intelligence, (AAAI-18)*, Sheila A. McIlraith and Kilian Q. Weinberger (Eds.). AAAI Press, 3–9.

[9] Jayaram Bhasker and Tariq Samad. 1991. The clique-partitioning problem. *Computers & Mathematics with Applications* 22, 6 (1991), 1–11.

[10] Paris Carbone, Asterios Katsifodimos, Stephan Ewen, Volker Markl, Seif Haridi, and Kostas Tzoumas. 2015. Apache Flink™: Stream and Batch Processing in a Single Engine. *IEEE Data Eng. Bull.* 38, 4 (2015), 28–38.

[11] Lu Chen, Chengfei Liu, Kewen Liao, Jianxin Li, and Rui Zhou. 2019. Contextual Community Search Over Large Social Networks. In *35th IEEE International Conference on Data Engineering, ICDE 2019*. IEEE, 88–99.

[12] Lu Chen, Chengfei Liu, Rui Zhou, Jianxin Li, Xiaochun Yang, and Bin Wang. 2018. Maximum Co-located Community Search in Large Scale Social Networks. *Proc. VLDB Endow.* 11, 10 (2018), 1233–1246.

[13] James Cheng, Yiping Ke, Ada Wai-Chee Fu, Jeffrey Xu Yu, and Linhong Zhu. 2010. Finding maximal cliques in massive networks by H*-graph. In *Proceedings of the ACM SIGMOD International Conference on Management of Data, SIGMOD 2010*, Ahmed K. Elmagarmid and Divyakant Agrawal (Eds.). ACM, 447–458.

[14] Peng Cheng, Hao Xin, and Lei Chen. 2017. Utility-Aware Ridesharing on Road Networks. In *Proceedings of the 2017 ACM International Conference on Management of Data, SIGMOD Conference 2017, Chicago, IL, USA, May 14-19, 2017*. ACM, 1197–1210.

[15] Peng Cheng, Hao Xin, and Lei Chen. 2017. Utility-aware ridesharing on road networks. In *Proceedings of the 2017 ACM International Conference on Management of Data*. ACM, 1197–1210.

[16] Deming Chu, Fan Zhang, Xuemin Lin, Wenjie Zhang, Ying Zhang, Yinglong Xia, and Chenyi Zhang. 2020. Finding the Best k in Core Decomposition: A Time and Space Optimal Solution. In *36th IEEE International Conference on Data Engineering, ICDE 2020*. IEEE, 685–696.

[17] Blerim Cici, Athina Markopoulou, and Nikolaos Laoutaris. 2015. Designing an on-line ride-sharing system. In *Proceedings of the 23rd SIGSPATIAL International Conference on Advances in Geographic Information Systems*. 60:1–60:4.

[18] Jean-François Cordeau. 2006. A branch-and-cut algorithm for the dial-a-ride problem. *Operations Research* 54, 3 (2006), 573–586.

[19] Jean-François Cordeau and Gilbert Laporte. 2003. The dial-a-ride problem (DARP): Variants, modeling issues and algorithms. *Quarterly Journal of the Belgian, French and Italian Operations Research Societies* 1, 2 (2003), 89–101.

[20] Jean-François Cordeau and Gilbert Laporte. 2003. A tabu search heuristic for the static multi-vehicle dial-a-ride problem. *Transportation Research Part B: Methodological* 37, 6 (2003), 579–594.

[21] Maximilien Danisch, Oana Balalau, and Mauro Sozio. 2018. Listing k-cliques in Sparse Real-World Graphs. In *Proceedings of the 2018 World Wide Web Conference on World Wide Web*, Pierre-Antoine Champin, Fabien Gandon, Mounia Lalmas, and Panagiotis G. Ipeirotis (Eds.). ACM, 589–598.

[22] Christos Giatsidis, Fragkiskos D. Malliaros, Dimitrios M. Thilikos, and Michalis Vazirgiannis. 2014. CoreCluster: A Degeneracy Based Graph Clustering Framework. In *Proceedings of the Twenty-Eighth AAAI Conference on Artificial Intelligence*, Carla E. Brodley and Peter Stone (Eds.). AAAI Press, 44–50.

[23] Lauri Häme. 2011. An adaptive insertion algorithm for the single-vehicle dial-a-ride problem with narrow time windows. *European Journal of Operational Research* 209, 1 (2011), 11–22.

[24] Xin Huang, Hong Cheng, Lu Qin, Wentao Tian, and Jeffrey Xu Yu. 2014. Querying k-truss community in large and dynamic graphs. In *International Conference on Management of Data, SIGMOD 2014*, Curtis E. Dyreson, Feifei Li, and M. Tamer Özsu (Eds.). ACM, 1311–1322.

[25] Yan Huang, Favyen Bastani, Ruoming Jin, and Xiaoyang Sean Wang. 2014. Large Scale Real-time Ridesharing with Service Guarantee on Road Networks. *PVLDB* 7, 14 (2014), 2017–2028.

[26] Yan Huang, Favyen Bastani, Ruoming Jin, and Xiaoyang Sean Wang. 2014. Large Scale Real-time Ridesharing with Service Guarantee on Road Networks. *Proc. VLDB Endow.* 7, 14 (2014), 2017–2028.

[27] Irina Ioachim, Jacques Desrosiers, Yvan Dumas, Marius M Solomon, and Daniel Villeneuve. 1995. A request clustering algorithm for door-to-door handicapped transportation. *Transportation science* 29, 1 (1995), 63–78.

[28] Svante Janson, Tomasz Łuczak, and Ilkka Norros. 2010. Large cliques in a power-law random graph. *Journal of Applied Probability* 47, 4 (2010), 1124–1135.

[29] Jang-Jei Jaw, Amedeo R Odoni, Harilaos N Psaraftis, and Nigel HM Wilson. 1986. A heuristic algorithm for the multi-vehicle advance request dial-a-ride problem with time windows. *Transportation Research Part B: Methodological* 20, 3 (1986), 243–257.

[30] Richard M. Karp. 1972. Reducibility Among Combinatorial Problems. In *Proceedings of a symposium on the Complexity of Computer Computations (The IBM Research Symposia Series)*, Raymond E. Miller and James W. Thatcher (Eds.). Plenum Press, New York, 85–103.

[31] Maksim Kitsak, Lazaros K Gallos, Shlomo Havlin, Fredrik Liljeros, Lev Muchnik, H Eugene Stanley, and Hernán A Makse. 2010. Identification of influential spreaders in complex networks. *Nature physics* 6, 11 (2010), 888–893.

[32] Jianxin Li, Xinjue Wang, Ke Deng, Xiaochun Yang, Timos Sellis, and Jeffrey Xu Yu. 2017. Most Influential Community Search over Large Social Networks. In *33rd IEEE International Conference on Data Engineering, ICDE 2017*. IEEE Computer Society, 871–882.

[33] Ye Li, Leong Hou U, Man Lung Yiu, and Ngai Meng Kou. 2017. An Experimental Study on Hub Labeling based Shortest Path Algorithms. *Proc. VLDB Endow.* 11, 4 (2017), 445–457.

[34] Zijian Li, Lei Chen, and Yue Wang. 2019. G*-Tree: An Efficient Spatial Index on Road Networks. In *35th IEEE International Conference on Data Engineering, ICDE 2019, Macao, China, April 8-11, 2019*. IEEE, 268–279.

[35] Zhe Lin, Fan Zhang, Xuemin Lin, Wenjie Zhang, and Zhihong Tian. 2021. Hierarchical Core Maintenance on Large Dynamic Graphs. *Proc. VLDB Endow.* 14, 5 (2021), 757–770.

[36] Qingyuan Linghu, Fan Zhang, Xuemin Lin, Wenjie Zhang, and Ying Zhang. 2020. Global Reinforcement of Social Networks: The Anchored Coreness Problem. In *Proceedings of the 2020 International Conference on Management of Data, SIGMOD Conference 2020, online conference*. ACM, 2211–2226.

[37] Shuo Ma, Yu Zheng, and Ouri Wolfson. 2013. T-share: A large-scale dynamic taxi ridesharing service. In *29th IEEE International Conference on Data Engineering, ICDE 2013*. 410–421.

[38] Shuo Ma, Yu Zheng, and Ouri Wolfson. 2015. Real-Time City-Scale Taxi Ridesharing. *IEEE Trans. Knowl. Data Eng.* 27, 7 (2015), 1782–1795.

[39] James Pan, Guoliang Li, and Juntao Hu. 2019. Ridesharing: Simulator, Benchmark, and Evaluation. *Proc. VLDB Endow.* 12, 10 (2019), 1085–1098.

[40] Symeon Papadopoulos, Yiannis Kompatsiaris, Athena Vakali, and Ploutarchos Spyridonos. 2012. Community detection in Social Media - Performance and application considerations. *Data Min. Knowl. Discov.* 24, 3 (2012), 515–554.

[41] Oleg Rokhlenko, Ydo Wexler, and Zohar Yakhini. 2007. Similarities and differences of gene expression in yeast stress conditions. *Bioinform.* 23, 2 (2007), 184–190.

[42] Douglas Oliveira Santos and Eduardo Candido Xavier. 2013. Dynamic Taxi and Ridesharing: A Framework and Heuristics for the Optimization Problem. In *IJCAI 2013, Proceedings of the 23rd International Joint Conference on Artificial Intelligence, Beijing, China, August 3-9, 2013*, Francesca Rossi (Ed.). IJCAI/AAAI, 2885–2891.

[43] Kijung Shin, Tina Eliassi-Rad, and Christos Faloutsos. 2016. Corescope: Graph mining using k-core analysis—patterns, anomalies and algorithms. In *2016 IEEE 16th international conference on data mining (ICDM)*. IEEE, 469–478.

[44] Yongxin Tong, Yuxiang Zeng, Zimu Zhou, Lei Chen, Jieping Ye, and Ke Xu. 2018. A Unified Approach to Route Planning for Shared Mobility. *PVLDB* 11, 11 (2018), 1633–1646.

[45] Jia Wang and James Cheng. 2012. Truss Decomposition in Massive Networks. *Proc. VLDB Endow.* 5, 9 (2012), 812–823.

[46] Jiachuan Wang, Peng Cheng, Libin Zheng, Chao Feng, Lei Chen, Xuemin Lin, and Zheng Wang. 2020. Demand-Aware Route Planning for Shared Mobility Services. *Proc. VLDB Endow.* 13, 7 (2020), 979–991.

[47] Kai Wang, Xin Cao, Xuemin Lin, Wenjie Zhang, and Lu Qin. 2018. Efficient Computing of Radius-Bounded k-Cores. In *34th IEEE International Conference on Data Engineering, ICDE 2018*. IEEE Computer Society, 233–244.

[48] Nigel HM Wilson, RW Weissberg, BT Higonnet, and J Hauser. 1975. *Advanced dial-a-ride algorithms*. Technical Report.

[49] Ka-Io Wong and Michael GH Bell. 2006. Solution of the Dial-a-Ride Problem with multi-dimensional capacity constraints. *International Transactions in Operational Research* 13, 3 (2006), 195–208.

[50] Yi Xu, Yongxin Tong, Yexuan Shi, Qian Tao, Ke Xu, and Wei Li. 2019. An Efficient Insertion Operator in Dynamic Ridesharing Services. In *35th IEEE International Conference on Data Engineering, ICDE 2019, Macao, China, April 8-11, 2019*. IEEE, 1022–1033.

[51] San Yeung, Evan Miller, and Sanjay Madria. 2016. A Flexible Real-Time Ridesharing System Considering Current Road Conditions. In *IEEE 17th International Conference on Mobile Data Management, MDM*. 186–191.

[52] Minji Yoon, Bryan Hooi, Kijung Shin, and Christos Faloutsos. 2019. Fast and Accurate Anomaly Detection in Dynamic Graphs with a Two-Pronged Approach. In *Proceedings of the 25th ACM SIGKDD International Conference on Knowledge Discovery & Data Mining, KDD 2019*, Ankur Teredesai, Vipin Kumar, Ying Li, Rómer Rosales, Evimaria Terzi, and George Karypis (Eds.). ACM, 647–657.

[53] Yuxiang Zeng, Yongxin Tong, Yuguang Song, and Lei Chen. 2020. The Simpler The Better: An Indexing Approach for Shared-Route Planning Queries. *Proc. VLDB Endow.* 13, 13 (2020), 3517–3530.

[54] Chen Zhang, Ying Zhang, Wenjie Zhang, Lu Qin, and Jianye Yang. 2019. Efficient Maximal Spatial Clique Enumeration. In *35th IEEE International Conference on Data Engineering, ICDE 2019*. IEEE, 878–889.

[55] Libin Zheng, Lei Chen, and Jieping Ye. 2018. Order dispatch in price-aware ridesharing. *Proceedings of the VLDB Endowment* 11, 8 (2018), 853–865.

[56] Libin Zheng, Peng Cheng, and Lei Chen. 2019. Auction-based order dispatch and pricing in ridesharing. In *2019 IEEE 35th International Conference on Data Engineering (ICDE)*. IEEE, 1034–1045.

A EFFECTS OF PENALTY AND BATCHING PERIOD.

Effect of penalty. Figure 13 represents the results of varying the penalty coefficient from 2 to 30. The experimental results show that the service rate of most methods does not influence by the varying penalty. pruneGDP, GAS and SARD, mainly takes the increased distance, the maximum group profit, and the shareability loss as their indicators in greedy strategies in the assignment phase, but the penalty coefficient will only affect them. However, RTV utilized the penalty coefficient in the constraint matrix of linear programming (LP), it will have a certain effect on the result of LP when the penalty coefficient is small, but the varying of penalty coefficient on RTV can be ignored when the penalty coefficient is large enough. In terms of unified cost, each experiment algorithm is proportional to the penalty coefficient. SARD still takes the lead in two datasets, with service rate increased by $8.55\% \sim 52.99\%$. Similarly, since the penalty coefficient does not affect the assignment phase, the execution time does not change obviously on two datasets.

Effect of batching period. Figure 14 represents the results of varying the batching period from 1 to 9 seconds for batch-based methods. The varying of batch time has little effect on the batch-based algorithms in terms of unified cost and service rate. SARD performs the best with the varying of batching period, which saves up to 44.18% and 53.08% in unified cost and increases the service rate with up to 29.2% and 48.96% in two datasets, respectively. For running time, since the number of execution rounds will decreases when the time period of each batch increases, the running times of these methods decrease. SARD is $5.17\times \sim 24.47\times$ faster than RTV and GAS.

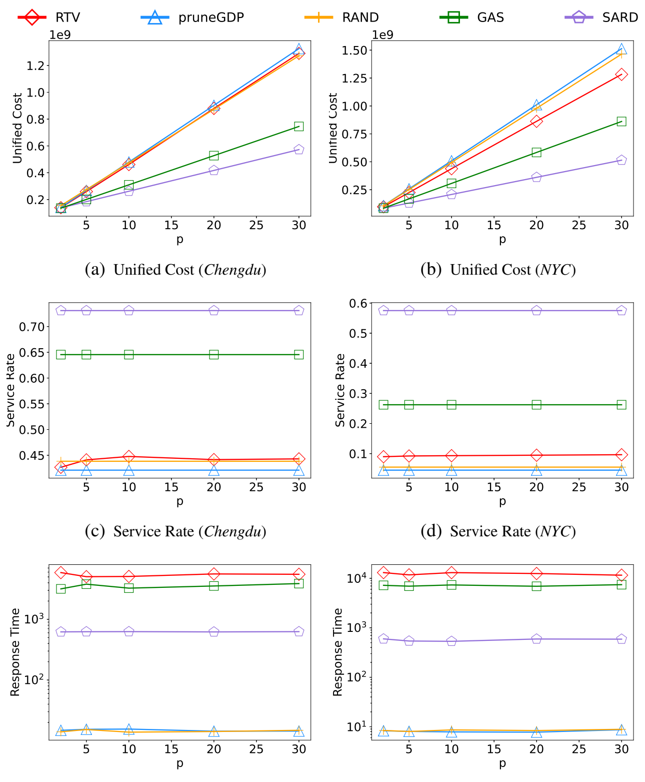

(a) Unified Cost (*Chengdu*) (b) Unified Cost (*NYC*)
(c) Service Rate (*Chengdu*) (d) Service Rate (*NYC*)
(e) Response Time (*Chengdu*) (f) Response Time (*NYC*)

Figure 13: Performance of varying p_r.

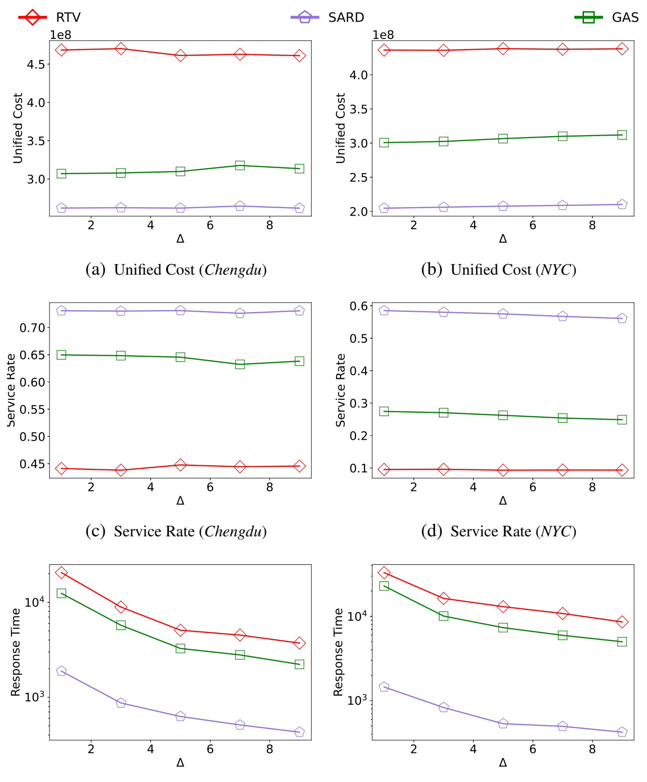

(a) Unified Cost (*Chengdu*) (b) Unified Cost (*NYC*)
(c) Service Rate (*Chengdu*) (d) Service Rate (*NYC*)
(e) Response Time (*Chengdu*) (f) Response Time (*NYC*)

Figure 14: Performance of varying Δ.